Supplemental Information

Figure S1

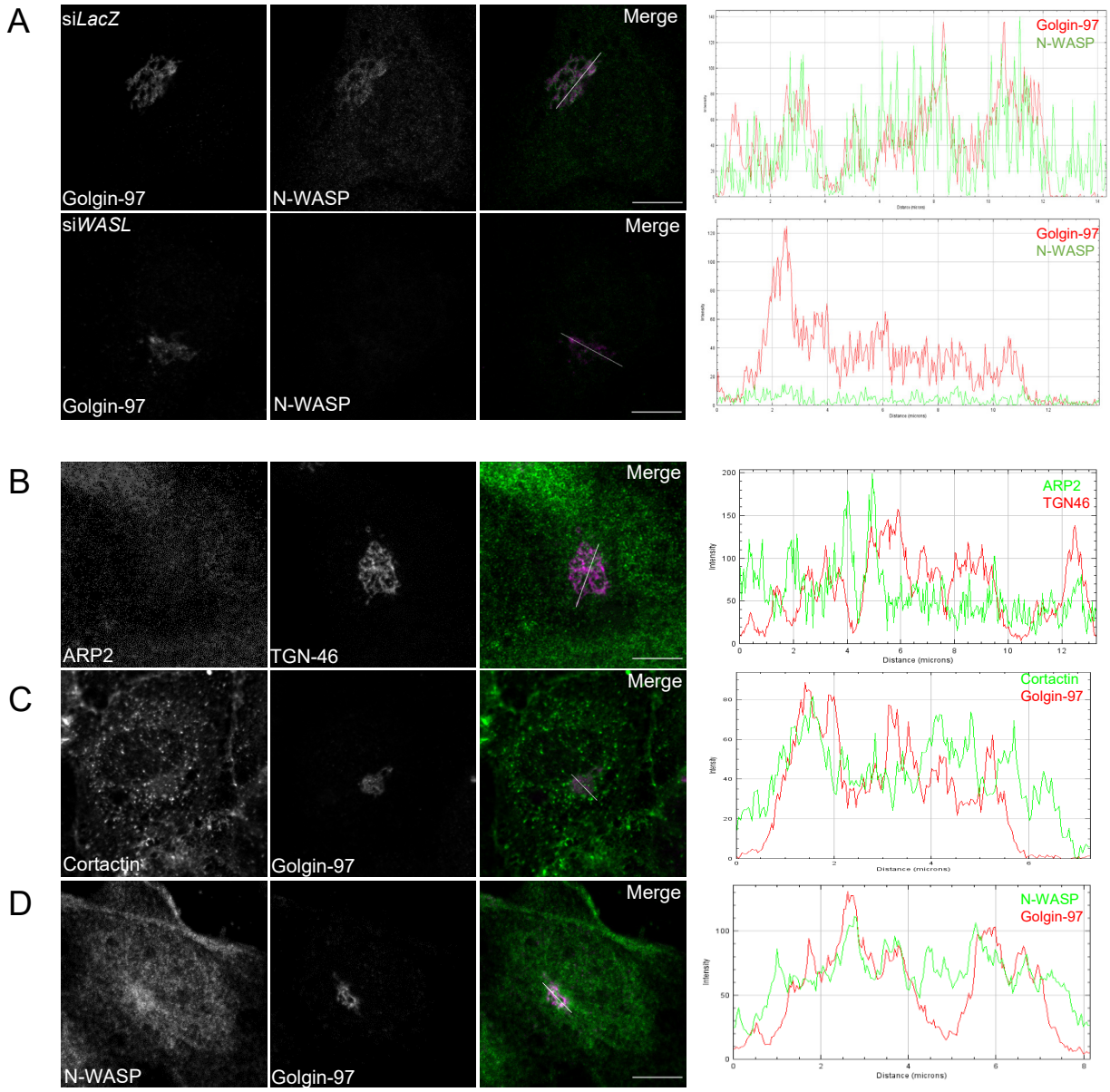

Fig. S1: (A) N-WASP antibody (ab126626) specificity control. HeLa cells were transfected with si*LACZ* or si*WASL*. After 48h cells were stained with anti-N-WASP and Golgin-97 antibodies. Image sections were acquired using a confocal laser scanning microscope. **(B)** ARP2 partially localizes to TGN46-positive structures. Confluent, differentiated HUVEC cell monolayers were stained for endogenous TGN-46 and Arp2. **(C)** Endogenous Cortactin partially localizes to Golgin-97-positive structures in confluent, differentiated HUVEC cell monolayers. **(D)** Endogenous N-WASP partially localizes to Golgin-97-positive structures in confluent differentiated HUVEC cell monolayers. **A-D**, all images depict single confocal sections. Line intensity profiles indicate co-localization. Scale bar*:* 10µm.

Figure S2

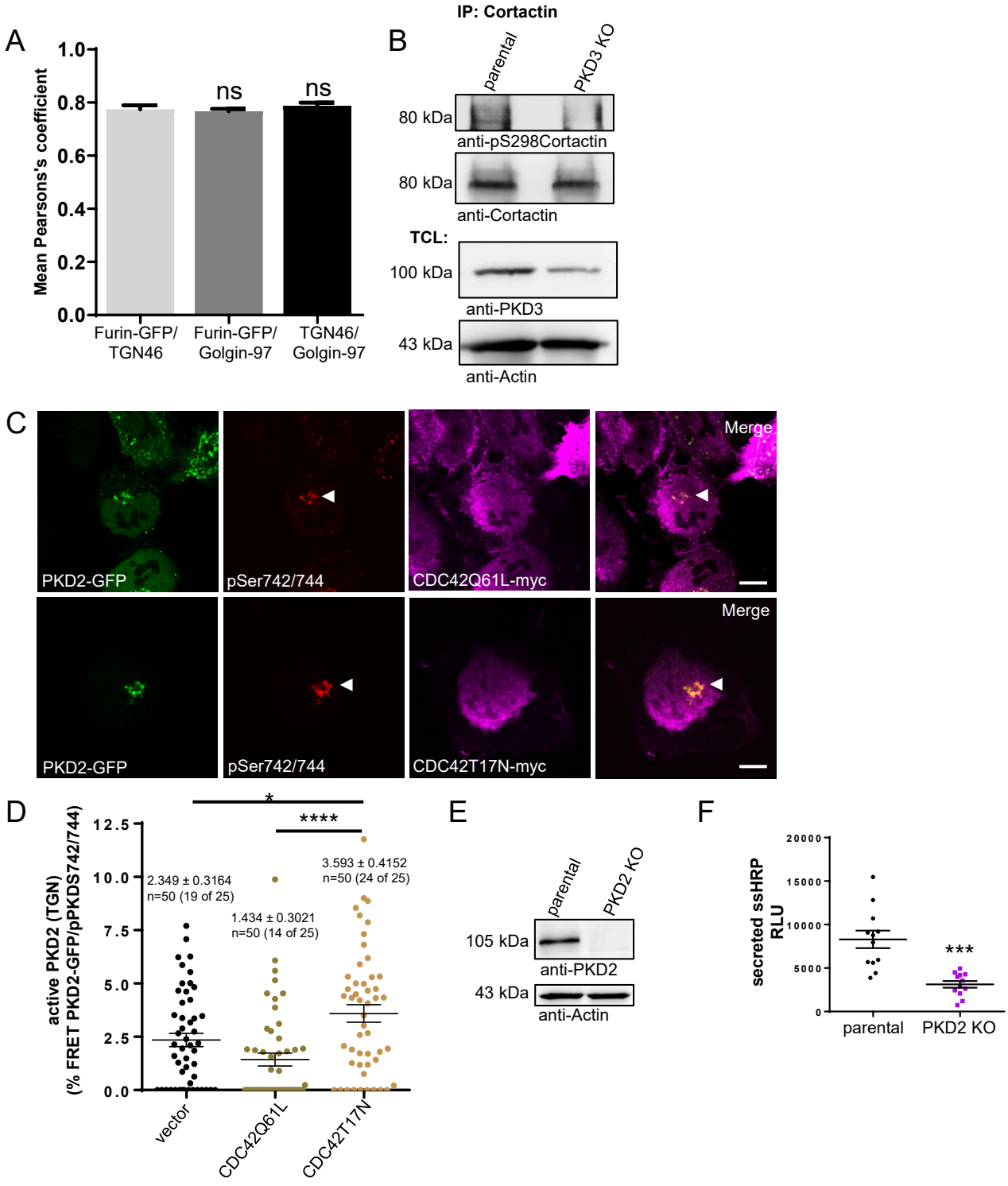

Fig. S2: (A) Quantitative co-localization of Furin-GFP with different TGN markers in HeLa cells. HeLa cells expressing Furin-GFP were stained for endogenous TGN-46 or Golgin-97, or HeLa cells were stained for both, TGN-46 and Golgin-97. The graph shows the mean Pearson's co-localization coefficient ± s.e.m. of three independent experiments from clipped TGN structures using rectangle ROIs around the TGN (n=15 cells). Statistical significance test: ANOVA with Tukey's post-test. ns, not significant. **(B)** PKD3 can phosphorylate endogenous Cortactin in HeLa cells. TCLs of HeLa parental and *PRKD3*-depleted CRISPR cells were subjected to IPs by precipitating endogenous Cortactin. Subsequently, phosphorylation of Cortactin at S298 was probed in Western blots by a specific anti-pS298-Cortactin antibody. IPs were re-probed for Cortactin expression. TCLs were probed for the expression of endogenous PKD3 to demonstrate CRISPR-mediated depletionOne exemplary experiment is depicted. **(C)** Co-expression of inactive CDC42T17N increases perinuclear PKD2 activity. HeLa cells were transfected with PKD2-GFP and vector or CDC42Q61L- and CDC42T17N-myc, respectively. Cells were stained for active PKD using the pPKDS742/744 activation loop antibody, while CDC42 constructs were stained using an anti-myc antibody. Scale bar*:* 10µm. **(D)** Quantitative AB-FRET analysis in cells from **C**. PKD2-GFP activity was probed by detecting FRET with the pPKDS742/744 activation loop antibody labeled with Alexa-568 secondary antibodies, whereas presence of ectopic CDC42 was identified using anti-myc and Alexa-647 antibodies. The graph shows mean ± s.e.m. %FRET of 25 cells and 2 equally sized ROIs used for mean of ROI analysis at PKD2-GFP-positive TGN-structures from three independent experiments (n=50 ROIs). Statistical test: ANOVA with Tukey's post-test. **(E)** Characterization *PRKD2* CRISPR KO cells. TCLs of HeLa parental and *PRKD2* CRISPR KO cells were probed for PKD2 expression. Actin was used as a loading control. **(F)** Knockout of *PRKD2* in HeLa cells reduces secretion of the artificial cargo HRP. Following 16h of ectopic ssHRP expression, HRP was collected in the culture supernatant for 4h and incubated with ECL solution. The graph shows mean ± s.e.m. of 12 independent experiments with four technical replica each. Statistical test: Two-tailed unpaired student's t-test.

Figure S3

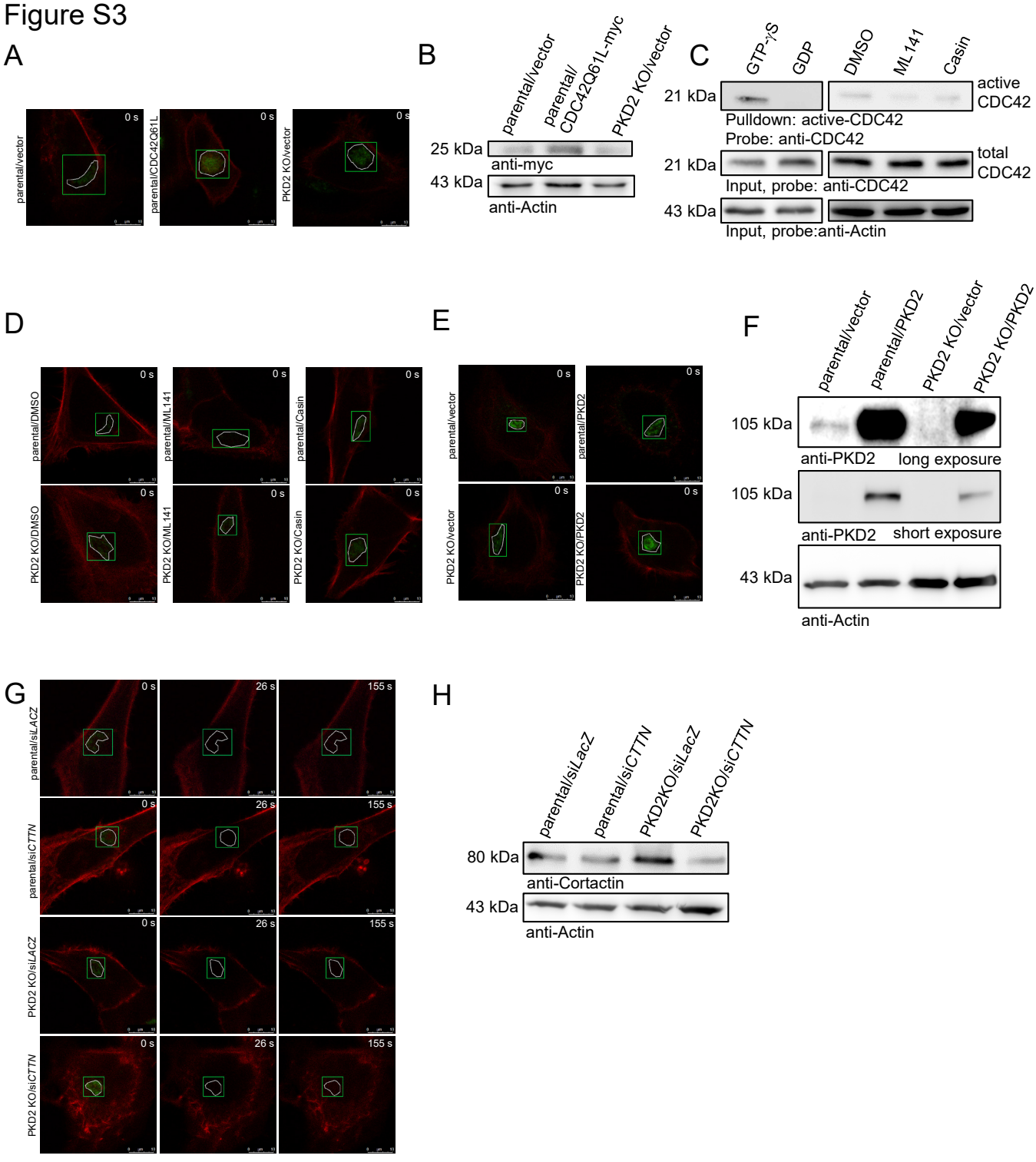

Fig. S3: (A) Exemplary images of cells detected for the indicated conditions in LifeAct-Ruby FRAP experiments in **Fig. 3E, F**. The bleach ROI is depicted in green, whereas the sub-ROI drawn around Furin-GFP-positive structures was used for quantification of steady-state F-actin at the TGN. **(B)** Exemplary expression of CDC42 in TCLs of HeLa cells as used for FRAP experiments in **Fig. 3E, F**. HeLa or HeLa PKD2 KO cells were transfected with Furin-GFP, LifeAct-Ruby and vector or CDC42Q61L-myc. **(C)** CDC42 activity assay. WI-38 cells were treated with DMSO, ML141 (10µM) or Casin (5µM) for 1h. Active CDC42-GTP was pulled down with PBD-beads. GTP-γ-S (1:5) and GDP-loaded CDC42 were used as respective controls. Protein bound to the beads was analyzed by Western Blot. **(D)** Exemplary images of cells detected for the indicated conditions in LifeAct-Ruby FRAP experiments in **Fig. 3G, H**. The bleach ROI is depicted in green, whereas the sub-ROI drawn around Furin-GFP-positive structures was used for quantification of steady-state F-actin at the TGN. **(E)** Exemplary images of cells detected for the indicated conditions in LifeAct-Ruby FRAP experiments in **Fig. 4A, B**. The bleach ROI is depicted in green, whereas the sub-ROI drawn around Furin-GFP-positive structures was used for quantification of steady-state F-actin at the TGN. **(F)** Exemplary expression of PKD2 in TCLs of HeLa cells as used in FRAP experiments in **Fig. 4A, B**. HeLa or HeLa PKD2 KO cells were transfected with Furin-GFP, LifeAct-Ruby and vector or PKD2 overexpression constructs. **(G)** Exemplary images of cells detected for the indicated conditions in LifeAct-Ruby FRAP experiments in **Fig. 4C, D**. T0, first pre-bleach image; T26, first post-bleach image; T155 last image of recovery series. The bleach ROI is depicted in green, whereas the sub-ROI drawn around Furin-GFP-positive structures was used for quantification of steady-state F-actin at the TGN. **(H)** Exemplary expression of Cortactin in TCLs of HeLa cells as used in FRAP experiments in **Fig. 4C, D**. HeLa or HeLa PKD2 KO cells were transfected with si*LACZ* or si*CTTN* and Furin-GFP as well as LifeAct-Ruby. After 48h cells were used for FRAP-experiments or generation of TCLs.

Figure S4

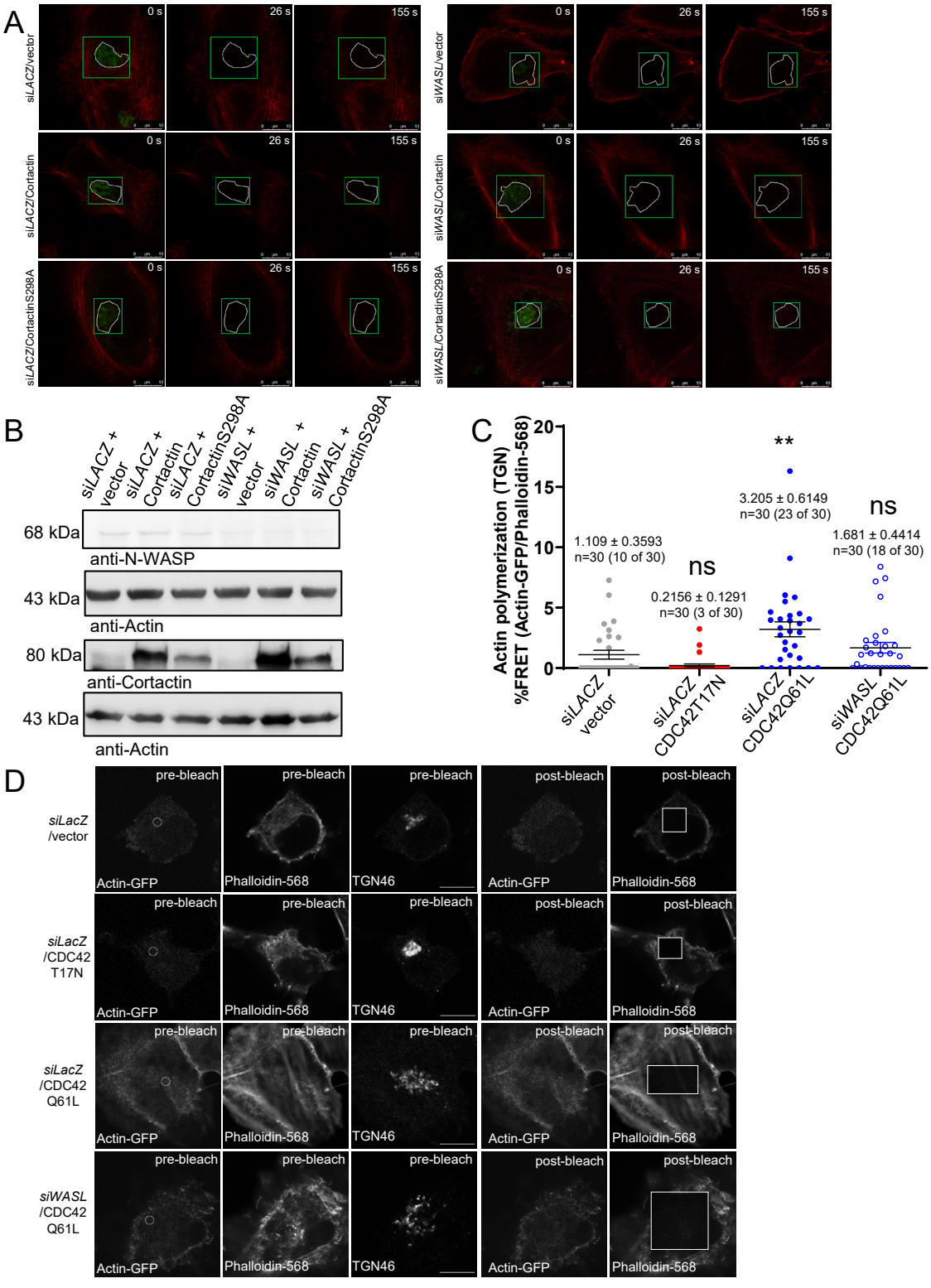

Fig. S4: (A) Exemplary images of cells detected for the indicated conditions in LifeAct-Ruby FRAP experiments in **Fig. 4E, F**. T0, first pre-bleach image; T26, first post-bleach image; T155 last image of recovery series. The bleach ROI is depicted in green, whereas the sub-ROI drawn around Furin-GFP-positive structures was used for quantification of steady-state F-actin at the TGN. **(B)** Exemplary expression of Cortactin and N-WASP in TCLs of HeLa cells as used in FRAP experiments in **Fig. 4E, F**. HeLa cells were transfected with si*LACZ* or si*WASL,* vector, Cortactin-FLAG or CortactinS298A-FLAG, Furin-GFP as well as LifeAct-Ruby. About 30h post transfection cells were analyzed by Western blotting. **(C)** Active CDC42Q61L enhances actin polymerization at the TGN in an N-WASP-dependent manner. Steady-state incorporation of Actin-GFP into Phalloidin-Alexa-568-labeled filaments was quantified by AB-FRET as a measure for relative actin polymerization. HeLa cells were co-transfected with si*LACZ* or si*WASL* and Actin-GFP as well as vector, CDC42T17N or CDC42Q61L, respectively. After 48h cells were processed for IF staining and labeled with Phalloidin-Alexa-568 as well as TGN46-Alexa-647. The graph shows mean ± s.e.m. %FRET of 30 cells with equally sized ROIs used for mean of ROI analysis at TGN-46-positive-Alexa-647-positive structures from three independent experiments (n=30 ROIs). Statistical test: ANOVA with Dunnett's post-test in respect to si*LACZ*/vector. **(D)** Exemplary images of AB-FRET experiments described in **C**. Left-hand side: Pre-bleach images of donor (Actin-GFP), acceptor (Phalloidin-Alexa-568), and the TGN46 as well as the ROI for intensity quantification are shown. Right-hand side: Post-bleach images of donor and acceptor with respective bleach ROIs. Scale bar: 10µm.

Figure S5

A

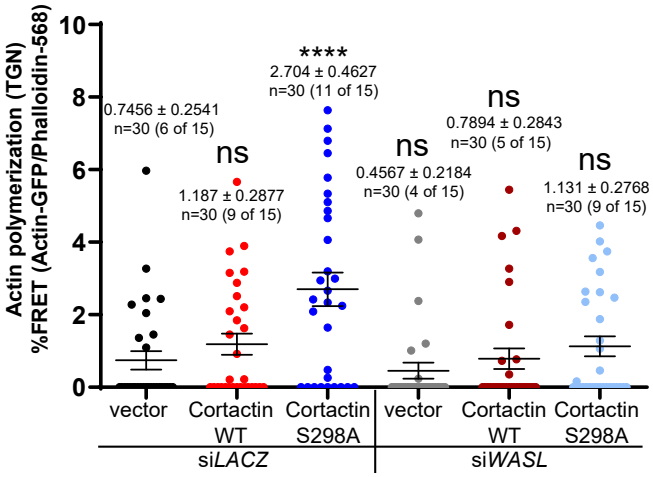

B

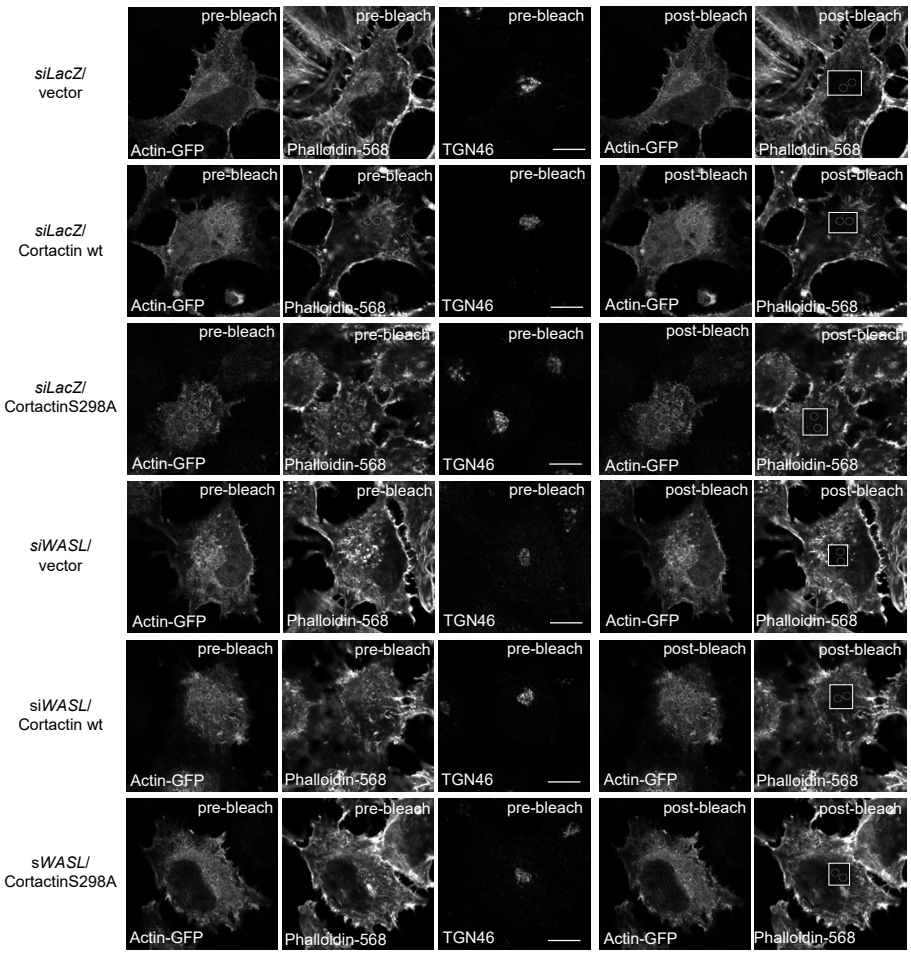

Fig. S5: (A) Non-phosphorylatable-CortactinS298A enhances actin polymerization at the TGN in an N-WASP-dependent manner. HeLa cells were co-transfected with si*LACZ* or si*WASL* and Actin-GFP as well as vector, Cortactin- or CortactinS298A-FLAG, respectively. After 48h cells were processed for IF staining and labeled with Phalloidin-Alexa-568 as well as TGN46-Alexa-647. The graph shows mean ± s.e.m. %FRET of 15 cells and 2 equally sized ROIs used for mean of ROI analysis at TGN46-positive TGN structures from three independent experiments (n=30 ROIs). Statistical significance test: ANOVA with Dunnett's post-test in respect to si*LACZ*/vector. **(B)** Exemplary images of AB-FRET experiments described in **A**. Left-hand side: Pre-bleach images of donor (Actin-GFP), acceptor (Phalloidin-Alexa-568), and the TGN46 (TGN marker) as well as the ROI for intensity quantification are shown. Right-hand side: Post-bleach images of donor and acceptor with respective bleach ROIs. Scale bar: 10µm.

Figure S6

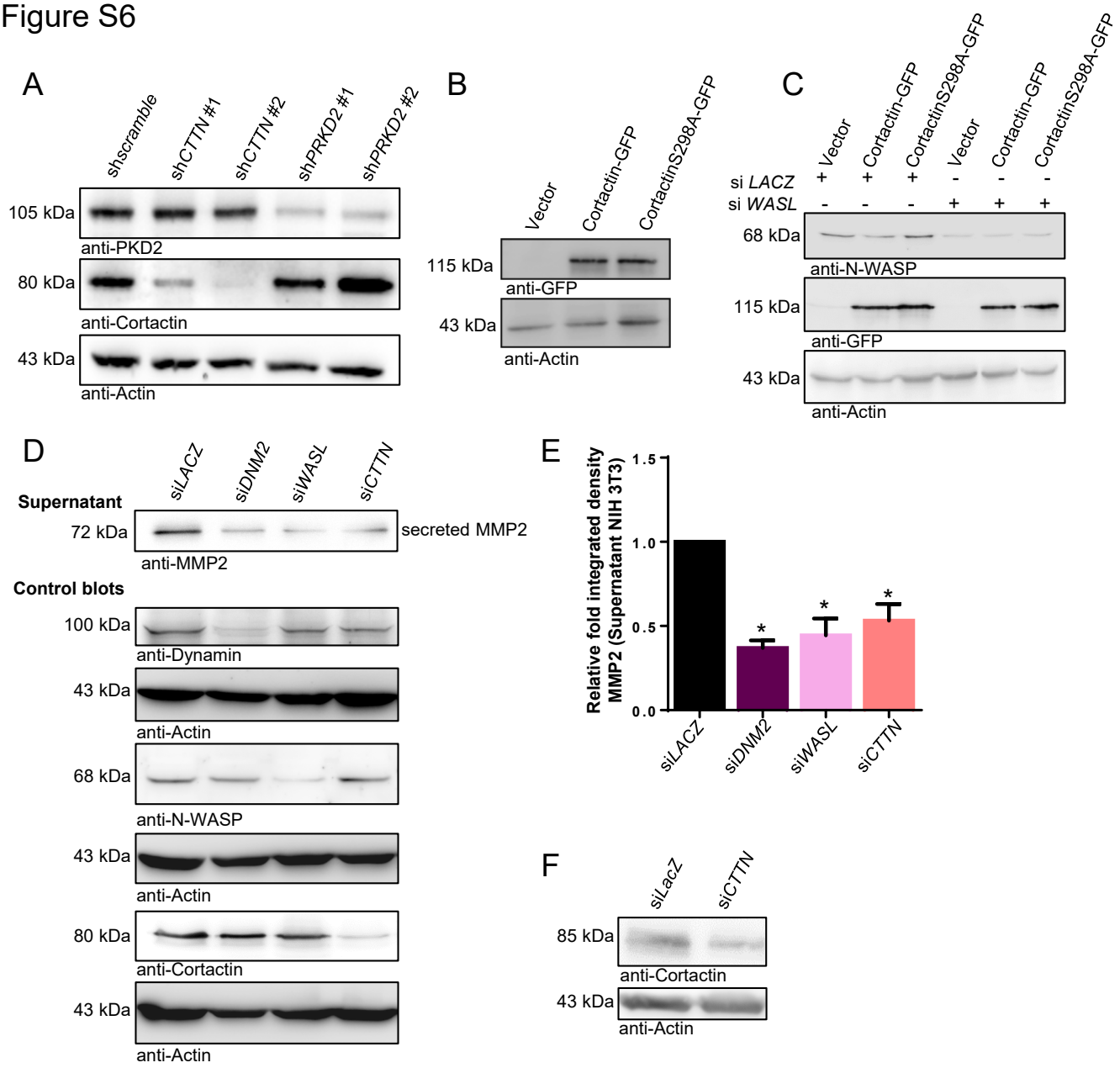

Fig. S6: (A) Knockdown of *CTTN* and *PRKD2* by two different shRNAs in semi-stable HEK293T cell lines used for HRP secretion assays in **Fig. 5A**. **(B)** Example of Cortactin- and CortactinS298A-GFP expression in transiently transfected HEK293T cell lines used for HRP secretion experiments in **Fig. 5B**. **(C)** Verification of the N-WASP knockdown and Cortactin- and CortactinS298A-GFP expression in transiently transfected HEK293T cell lines used for HRP secretion experiments in **Fig. 5E**. **(D)** Depletion of Dynamin2, N-WASP and Cortactin impairs secretion of endogenous MMP2 from NIH 3T3 fibroblasts. NIH 3T3 cells transfected with si*LACZ*, si*DNM2*, si*WASL* and si*CTTN*. After 48h, MMP2 was accumulated in 900µl of serum-free media for 24h. Supernatants analyzed by Western blot for the presence of MMP2 and TCLs for knockdown of Dynamin, N-WASP and Cortactin, respectively. One exemplary experiment of four is shown. **(E)** Statistical analysis of Western blots from **D**. The graph shows mean ± s.e.m. of four independent experiments. Statistical test: ANOVA with Dunnett's post-test towards si*LACZ*. **(F)** Exemplary Western blot show depletion of Cortactin in WI38 pulmonary fibroblasts used in **Fig. 5F, G**.

Figure S7

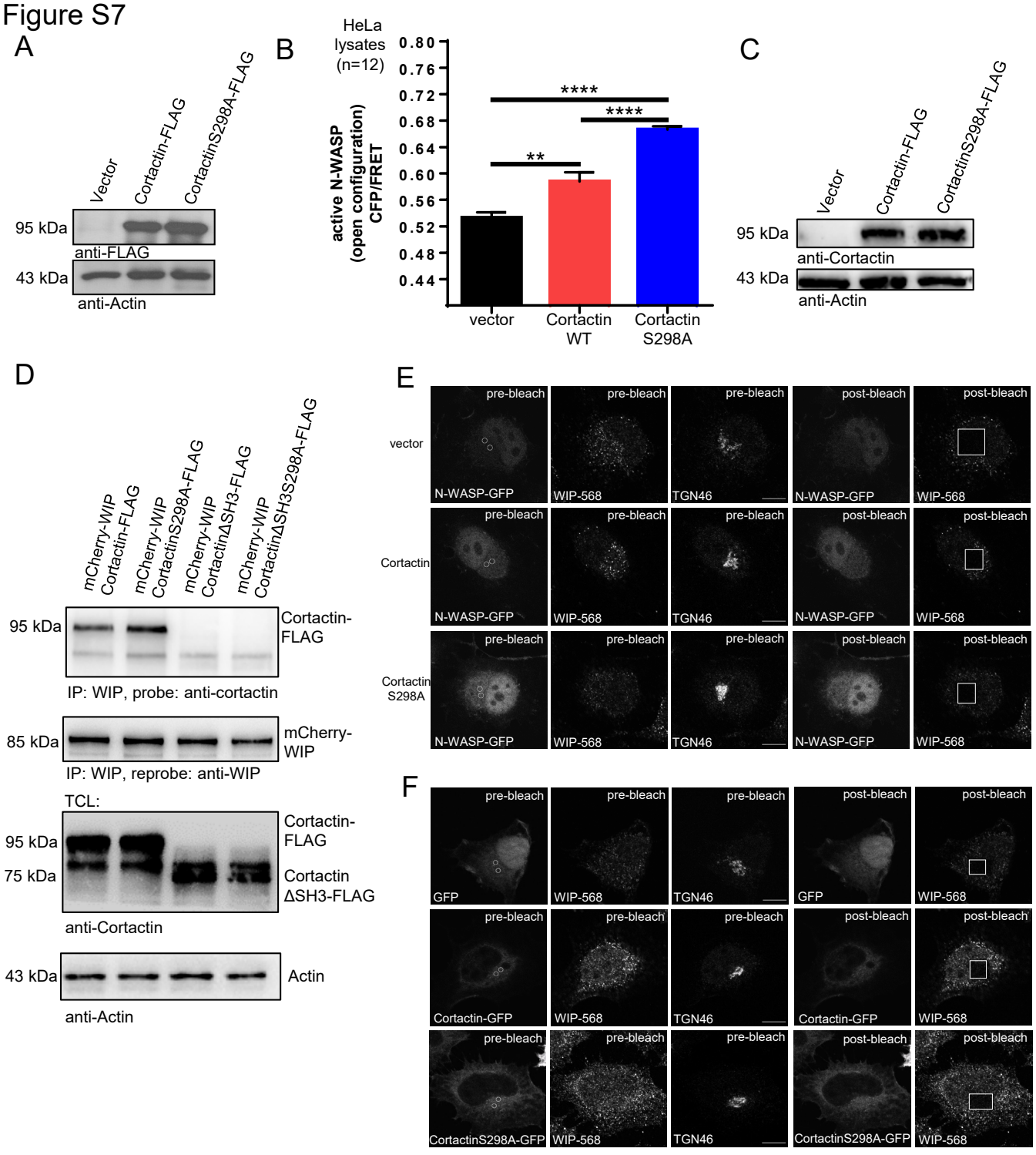

Fig. S7: (A) Expression of Cortactin- and CortactinS298A-FLAG in HEK293T TCLs used for N-WASP-FRET biosensor measurements in **Fig. 6A**. **(B)** Expression of CortactinS298A significantly activates N-WASP in respect to wildtype Cortactin or vector control in HeLa cells. The N-WASP biosensor was co-transfected with the indicated constructs (1:3). After 24h, cells were lysed and fluorescence was measured in cleared lysates using a plate reader. The graph displays relative CFP/FRET ratios for n=12 independently transfected samples. **(C)** Expression of Cortactin- and CortactinS298A-FLAG in HeLa cell lysates used for N-WASP-FRET biosensor measurements in **B**. **(D)** Binding of WIP to Cortactin is enhanced for the non-phosphorylatable-S298A-mutant and dependent on the Cortactin-SH3-domain. HEK293T cells expressing mCherry-WIP and Cortactin-FLAG, CortactinS298A-FLAG, CortactinΔSH3-FLAG or CortactinΔSH3S298A-FLAG were subjected to CoIPs by precipitating WIP, ectopically expressed Cortactin was detected. IPs were re-probed with anti-WIP antibody. The lower panel shows TCLs probed for the expression of the different Cortactin-FLAG constructs. One exemplary experiment is shown. **(E)** Exemplary images of AB-FRET experiments described in **Fig. 7G**. Left-hand side: Pre-bleach images of donor (N-WASP-GFP), acceptor (WIP-Alexa-568), and the TGN46 as well as the ROI for intensity quantification are shown. Right-hand side: Post-bleach images of donor and acceptor with respective bleach ROIs. Scale bar: 10µm. **(F)** Exemplary images of AB-FRET experiments described in **Fig. 7H**. Left-hand side: Pre-bleach images of donor (GFP, Cortactin-GFP, CortactinS298A-GFP), acceptor (WIP-Alexa-568), and the TGN46 as well as the ROI for intensity quantification are shown. Right-hand side: Post-bleach images of donor and acceptor with respective bleach ROIs. Scale bar: 10µm.

Figure S8

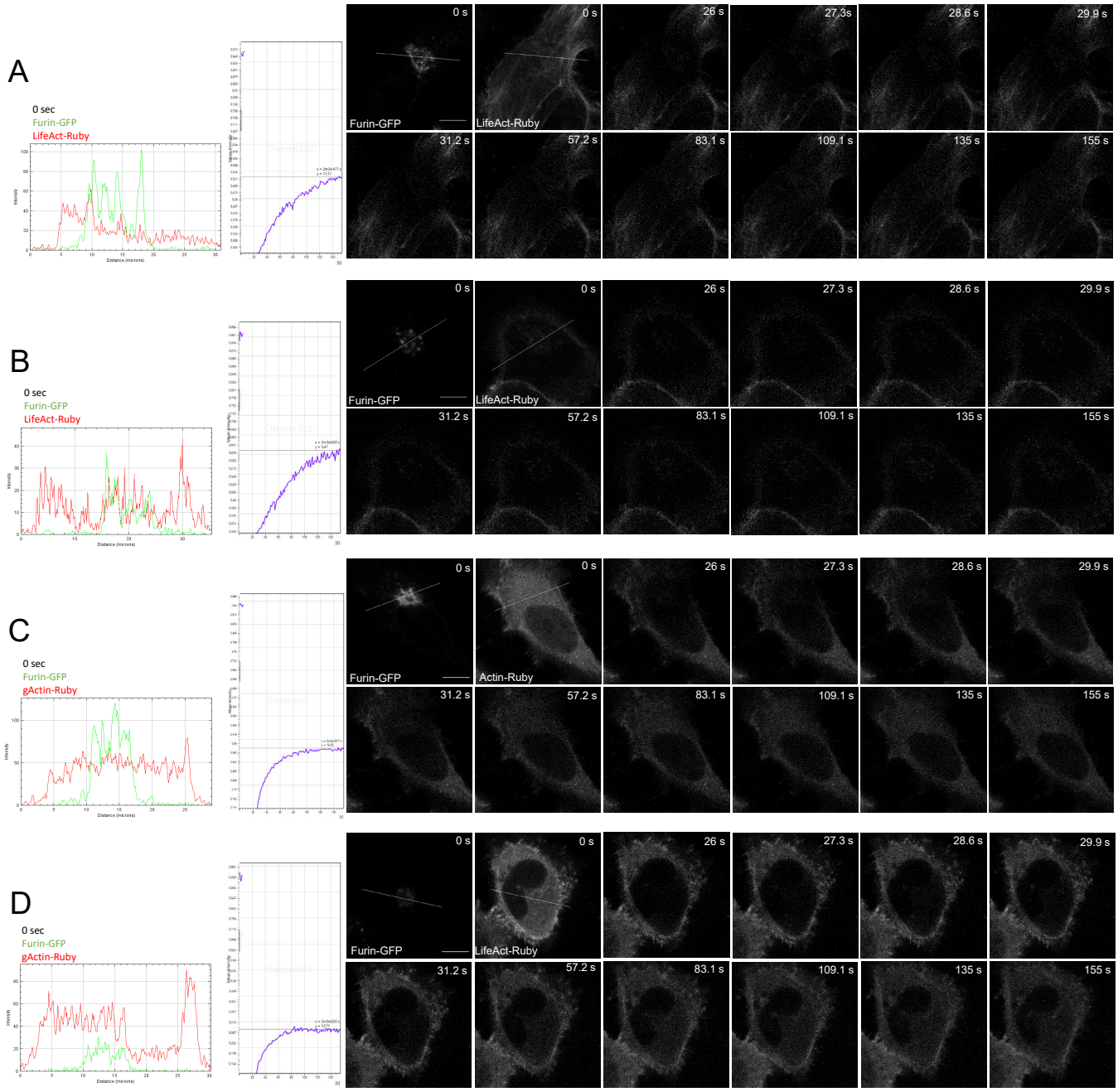

Fig. S8: (A) FRAP curve and respective images of a HeLa cell transfected with plasmids for Furin-GFP, LifeAct-Ruby and vector. **(B)** FRAP curve and respective images of a HeLa cell transfected with plasmids for Furin-GFP, LifeAct-Ruby and CDC42Q61L. **(C)** FRAP curve and respective images of a HeLa cell transfected with plasmids for Furin-GFP, Actin-Ruby and pcDNA vector as control. **(D)** FRAP curve and respective images of a HeLa cell transfected with plasmids for Furin-GFP, Actin-Ruby and CDC42Q61L.

Supplementary movies

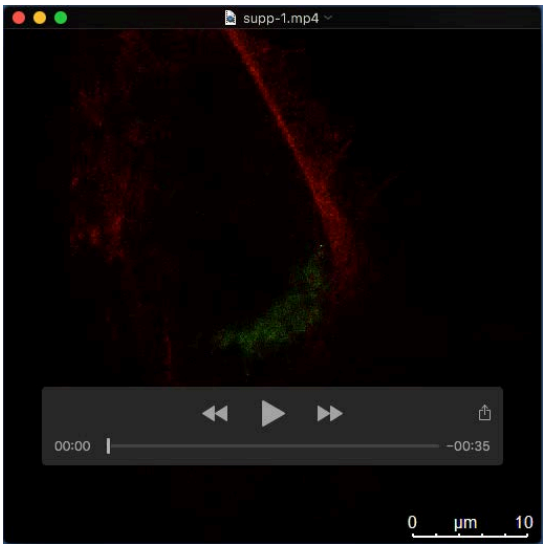

Movie 1. LifeAct-Ruby-FRAP to measure steady-state F-actin formation at the TGN in a HeLa parental/vector control cells. Cells were co-transfected with LifeAct-RubyN143C, Furin-GFP (TGN marker) and the indicated constructs. Images were acquired using a Leica TSC-SP8-HCS confocal laser scanning microscope. Five pre-bleach images; fluorescence recovery: 100 images (130s). Relative-time stamps and scale bar are included in the video sequence.

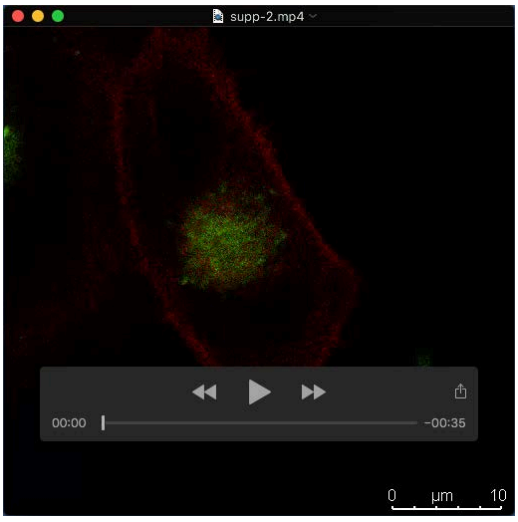

Movie 2. LifeAct-Ruby-FRAP to measure steady-state F-actin formation at the TGN in a HeLa parental/CDC42Q61L cell. Cells were co-transfected with LifeAct-RubyN143C, Furin-GFP (TGN marker) and the indicated constructs. Images were acquired using a Leica TSC-SP8-HCS confocal laser scanning microscope. Five pre-bleach images; fluorescence recovery: 100 images (130s). Relative-time stamps and scale bar are included in the video sequence.

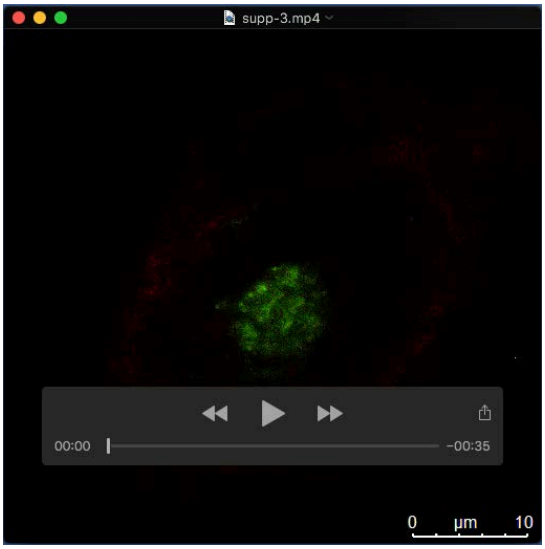

Movie 3. LifeAct-Ruby-FRAP to measure steady-state F-actin formation at the TGN in a HeLa PKD2KO/vector cell. Cells were co-transfected with LifeAct-RubyN143C, Furin-GFP (TGN marker) and the indicated constructs. Images were acquired using a Leica TSC-SP8-HCS confocal laser scanning microscope. Five pre-bleach images; fluorescence recovery: 100 images (130s). Relative-time stamps and scale bar are included in the video sequence.

Movie 4. LifeAct-Ruby-FRAP to measure steady-state F-actin formation at the TGN in a HeLa parental/vector cell. Cells were co-transfected with LifeAct-RubyN143C, Furin-GFP (TGN marker) and the indicated constructs. Images were acquired using a Leica TSC-SP8-HCS confocal laser scanning microscope. Five pre-bleach images; fluorescence recovery: 100 images (130s). Relative-time stamps and scale bar are included in the video sequence.

Journal of Cell Science • Supplementary information

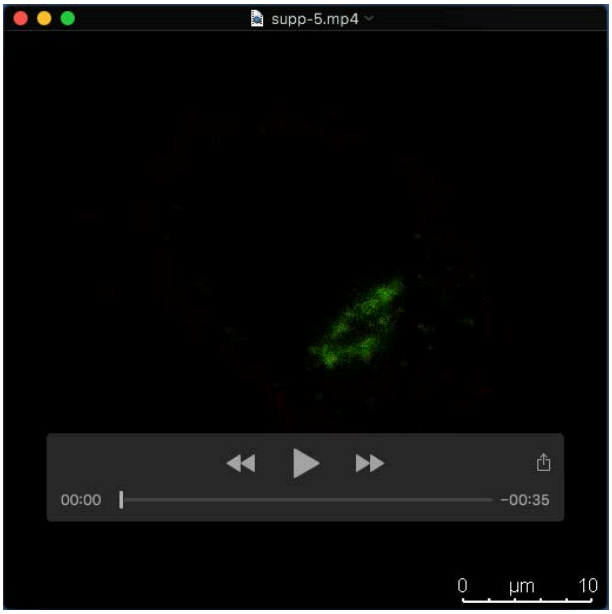

Movie 5. LifeAct-Ruby-FRAP to measure steady-state F-actin formation at the TGN in a HeLa parental/PKD2 cell. Cells were co-transfected with LifeAct-RubyN143C, Furin-GFP (TGN marker) and the indicated constructs. Images were acquired using a Leica TSC-SP8-HCS confocal laser scanning microscope. Five pre-bleach images; fluorescence recovery: 100 images (130s). Relative-time stamps and scale bar are included in the video sequence.

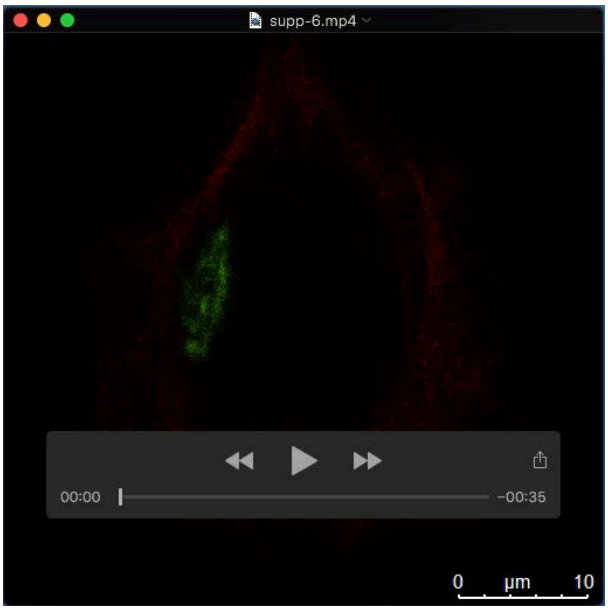

Movie 6. LifeAct-Ruby-FRAP to measure steady-state F-actin formation at the TGN in a HeLa PKD2KO/vector cell. Cells were co-transfected with LifeAct-RubyN143C, Furin-GFP (TGN marker) and the indicated constructs. Images were acquired using a Leica TSC-SP8-HCS confocal laser scanning microscope. Five pre-bleach images; fluorescence recovery: 100 images (130s). Relative-time stamps and scale bar are included in the video sequence.

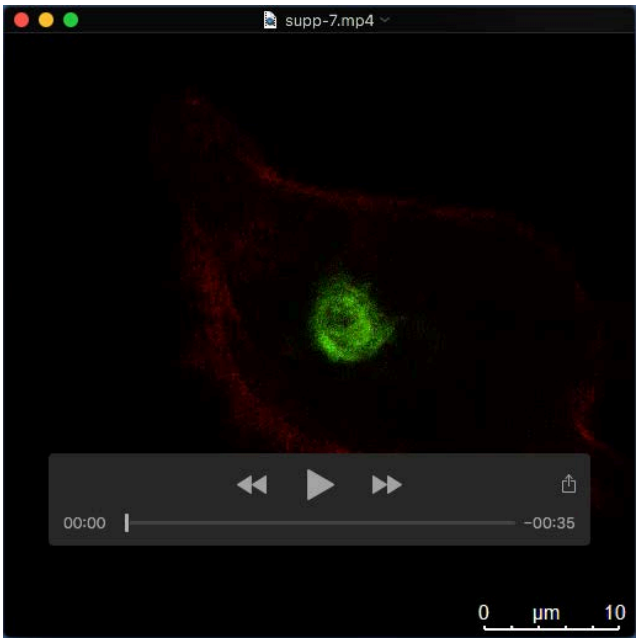

Movie 7. LifeAct-Ruby-FRAP to measure steady-state F-actin formation at the TGN in a HeLa PKD2KO/PKD2 cell. Cells were co-transfected with LifeAct-RubyN143C, Furin-GFP (TGN marker) and the indicated constructs. Images were acquired using a Leica TSC-SP8-HCS confocal laser scanning microscope. Five pre-bleach images; fluorescence recovery: 100 images (130s). Relative-time stamps and scale bar are included in the video sequence.

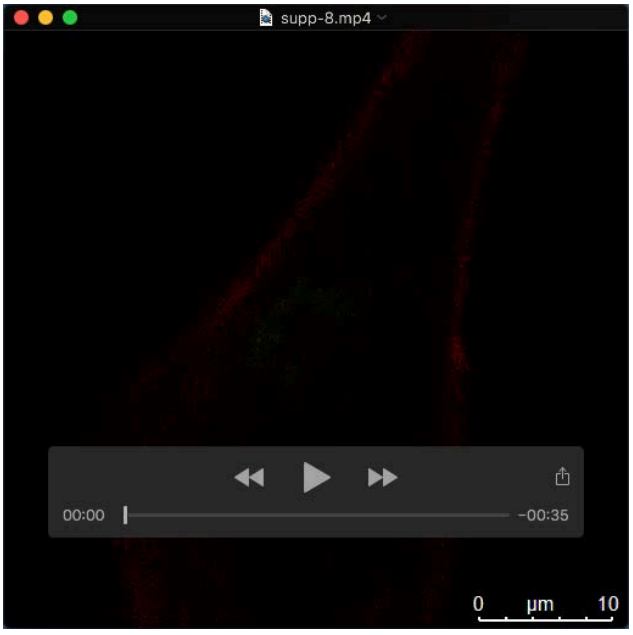

Movie 8. LifeAct-Ruby-FRAP to measure steady-state F-actin formation at the TGN in a HeLa parental/si*LACZ* cell. Cells were co-transfected with LifeAct-RubyN143C, Furin-GFP (TGN marker) and the indicated constructs or siRNAs. After incubation for 48h, images were acquired using a Leica TSC-SP8-HCS confocal laser scanning microscope. Five pre-bleach images; fluorescence recovery: 100 images (130s). Relative-time stamps and scale bar are included in the video sequence.

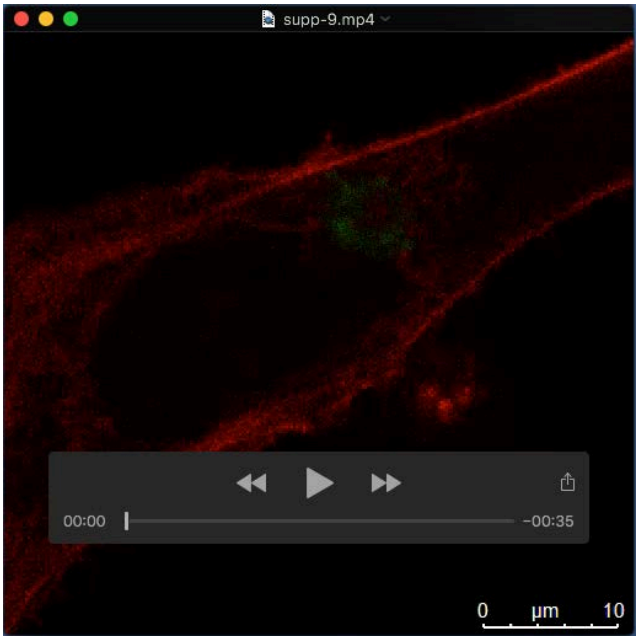

Movie 9. LifeAct-Ruby-FRAP to measure steady-state F-actin formation at the TGN in a HeLa parental/si*CTTN* cell. Cells were co-transfected with LifeAct-RubyN143C, Furin-GFP (TGN marker) and the indicated constructs or siRNAs. After incubation for 48h, images were acquired using a Leica TSC-SP8-HCS confocal laser scanning microscope. Five pre-bleach images; fluorescence recovery: 100 images (130s). Relative-time stamps and scale bar are included in the video sequence.

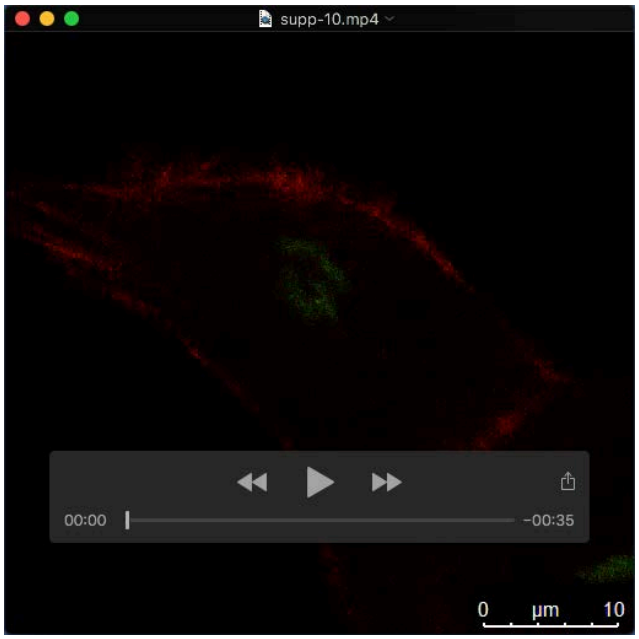

Movie 10. LifeAct-Ruby-FRAP to measure steady-state F-actin formation at the TGN in a HeLa PKD2KO/si*LACZ* cell. Cells were co-transfected with LifeAct-RubyN143C, Furin-GFP (TGN marker) and the indicated constructs or siRNAs. After incubation for 48h, images were acquired using a Leica TSC-SP8-HCS confocal laser scanning microscope. Five pre-bleach images; fluorescence recovery: 100 images (130s). Relative-time stamps and scale bar are included in the video sequence.

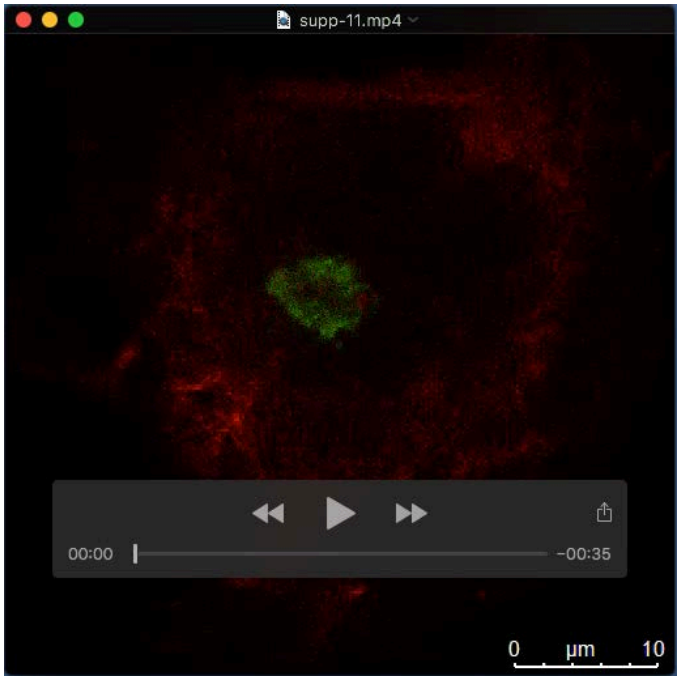

Movie 11. LifeAct-Ruby-FRAP to measure steady-state F-actin formation at the TGN in a HeLa PKD2KO/si*CTTN* cell. Cells were co-transfected with LifeAct-RubyN143C, Furin-GFP (TGN marker) and the indicated constructs or siRNAs. After incubation for 48h, images were acquired using a Leica TSC-SP8-HCS confocal laser scanning microscope. Five pre-bleach images; fluorescence recovery: 100 images (130s). Relative-time stamps and scale bar are included in the video sequence.

Table S1: List of primary and secondary antibodies with ordering numbers, companies and concentrations.

Name	Ordering number	Company	Dilution
Actin	#A5441	Sigma Aldrich, (Taufkirchen, Germany)	WB: 1:2000
Alexa-Fluor 488/568/647 goat-anti-mouse	#A11031 #A11001 #A21235	Thermo Scientific, St. Leon-Rot, Germany	IF: 1:400
Alexa-Fluor 488/568/647 goat-anti-rabbit	# A11034 # A11011 # A21244	Thermo Scientific, St. Leon-Rot, Germany	IF: 1:400
ARP2	#sc-376698	Santa Cruz Biotechnology, Heidelberg, Germany	IF: 1:100 PLA: 1:50
Cortactin (H-191)	#sc-11408	Santa Cruz Biotechnology, Heidelberg, Germany	WB: 1:1000 IF: 1:100 PLA: 1:100
Cortactin (H-5)	#sc-55579	Santa Cruz Biotechnology, Heidelberg, Germany Biotechnology, Heidelberg, Germany	PLA: 1:50
pS298Cortactin	was kindly provided by Johan van Lint, Leuven, Belgium	(De Kimpe et al., 2009)	WB: 1:500
Dynamin	#sc-11362	Santa Cruz Biotechnology, Heidelberg, Germany	WB: 1:1000 IF: 1:100
Flag-M2	#F1804	Sigma Aldrich, Taufkirchen, Germany	WB: 1:2000 IF: 1:100
GFP	#11814460 001	Roche, Basel, Switzerland	WB: 1:2000
Golgin-97	#A21270	Thermo Scientific, St. Leon-Rot, Germany	IF: 1:400

MMP2	#ab37150	Abcam, Cambridge, UK	WB: 1:1000
MMP-2 (D4M2N)	#40994	Cell Signaling Technology, Danvers, USA	IF: 1:100
Myc (9E10)	MABE282	Merck, Darmstadt, Germany	WB: 1:1000 IF: 1:400
N-WASP	#48483	Cell Signaling Technology, Danvers, USA	WB: 1:1000
N-WASP	#ab126626	Abcam, Cambridge, UK	IF: 1:50 PLA: 1:50
PKD2	ST1042	Merck, Darmstadt, Germany	WB: 1:1000
pPKDS742/744	#2054	Cell Signaling Technology, Danvers, USA	IF: 1:100
pPKDS916	#2051	Cell Signaling Technology, Danvers, USA	WB: 1:2000 IF: 1:100
TGN-46	#AP326910SU-N	Acris (OriGene Technologies, Rockville, MD, USA)	IF: 1:400
WIP (A-7)	#sc-271113	Santa Cruz Biotechnology, Heidelberg, Germany	IF: 1:100 WB: 1:1000
WIP (C-1)	#sc-390099	Santa Cruz Biotechnology, Heidelberg, Germany	WB: 1:1000 IP: 2.5µg/sample

References

De Kimpe, L., Janssens, K., Derua, R., Armacki, M., Goicoechea, S., Otey, C., Waelkens, E., Vandoninck, S., Vandenheede, J. R., Seufferlein, T. et al. (2009). Characterization of cortactin as an in vivo protein kinase D substrate: interdependence of sites and potentiation by Src. *Cell Signal* **21**, 253-63.

Table S2: List of cDNA expression vectors, shRNAs, siRNAs and sequencing primers

Name	Source	Reference
cDNA expression vectors		
pCR3.V62-Met-Flag-Cortactin	A. Hausser, University of Stuttgart, Germany	(Eiseler et al., 2010)
pCR3.V62-Met-Flag-CortactinS298A	A. Hausser, University of Stuttgart, Germany	(Eiseler et al., 2010)
pcDNA3-FLAG-CortactinΔSH3	this study	
pcDNA3-FLAG-CortactinΔSH3-S298A	this study	
pEGFP-N1-Cortactin	A. Hausser, University of Stuttgart, Germany	(Eiseler et al., 2010)
pEGFP-N1-CortactinS298A	A. Hausser, University of Stuttgart, Germany	(Eiseler et al., 2010)
N-WASP-GFP	Ralf Kemkemer, Max Planck Institute for Medical Research	-
pEGFP-N1-PKD2	A. Hausser, University of Stuttgart, Germany	(Hausser et al., 2002; Hausser et al., 2005; Wille et al., 2014)
pmRuby-Actin7	F. Oswald, Ulm University, Germany	
pcDNA3-LifeAct-mRubyN143C	F. Oswald, Ulm University, Germany	
Furin-GFP	T. Seufferlein, Ulm University, Germany	
pRK5-myc-Cdc42Q61L	Addgene No: 12974	
pRK5-myc-Cdc42T17N	Addgene No: 12973	
pcDNA3-PKD2	A. Hausser, University of Stuttgart, Germany	(Hausser et al., 2002; Hausser et al., 2005; Wille et al., 2014)
CFP-N-WASP-YFP FRET activity sensor	John Condeelis, Albert-Einstein College of Medicine, NY, USA	(Lorenz et al., 2004)
pmCherry-C1 hWIP	Addgene No: 29573	(Cortesio et al., 2010)
siRNAs		

si*LacZ* 5‘-GCGGCUGCCGGAAUUUACC-3‘	Eurofins Genomics, Ebersberg, Germany	(Eiseler et al., 2010; Wille et al., 2014; Ziegler et al., 2011)
si*WASL* (Hs_*WASL*_6) cat.: SI02664263 5’-GAUACGACAGGGUAUCCAAtt-3’	Quiagen, Hilden, Germany	
si*PRKD*2 (s24646), cat.: 4390824 5‘-AGAUGAUCCUGUCCAGUGAtt-3‘	Thermo Scientific, St. Leon-Rot, Germany	
si*CTTN,* human (s4667), cat.: 4392420 5‘-CCAACAUCGAGAUGAUUGAtt-3‘	Thermo Scientific, St. Leon-Rot, Germany	
si*DMN2* (s65068), cat.: 4390815 5’-GGACCUUCGACAGAUUGAAtt-3’	Thermo Scientific, St. Leon-Rot, Germany	
si*CTTN*, mouse (s64627), cat.: 4390771 5’-GAAUCCCAAAAAGACUAUAtt-3’	Thermo Scientific, St. Leon-Rot, Germany	
si*WASL*, mouse (s91559), cat.: 4390771 5’-GGGAUGCGCUUUUAGACCAtt-3’	Thermo Scientific, St. Leon-Rot, Germany	
shRNA		
pLKO.1-puro sh *scramble* (Mission shRNA, Sigma shc002)	Sigma Aldrich, Taufkirchen, Germany	
shCTTN #1: pLKO.1-puro sh *CTTN* (NM_005231, TRCN0000040274)	Thermo Scientific, St. Leon-Rot, Germany	
sh*CTTN* #2: pLKO.1-puro sh *CTTN* (NM_005231, TRCN0000040273)	Thermo Scientific, St. Leon-Rot, Germany	
shPRKD2 #1 pLKO.1-puro sh *PRKD2* (NM_016457.x-1720s1c1)	Sigma Aldrich, Taufkirchen, Germany	
sh*PRKD2* #2 pLKO.1-puro sh *PRKD2* (NM_016457.x-294s1c1)	Sigma Aldrich, Taufkirchen, Germany	
Genomic sequencing primer		
PRKD2 sequencing forward primer: 5‘ GAAGGCGGCTCTGAGCTTTTC 3‘	biomers.net, Ulm, Germany	
PRKD2 sequencing reverse primer: 5’ GCCACCACCTCTCACCCGACAG 3’	biomers.net, Ulm, Germany	

References

Cortesio, C. L., Perrin, B. J., Bennin, D. A. and Huttenlocher, A. (2010). Actin-binding protein-1 interacts with WASp-interacting protein to regulate growth factor-induced dorsal ruffle formation. *Mol Biol Cell* **21**, 186-97.

Eiseler, T., Hausser, A., De Kimpe, L., Van Lint, J. and Pfizenmaier, K. (2010). Protein kinase D controls actin polymerization and cell motility through phosphorylation of cortactin. *J Biol Chem* **285**, 18672-83.

Hausser, A., Link, G., Bamberg, L., Burzlaff, A., Lutz, S., Pfizenmaier, K. and Johannes, F. J. (2002). Structural requirements for localization and activation of protein kinase C mu (PKC mu) at the Golgi compartment. *J Cell Biol* **156**, 65-74.

Hausser, A., Storz, P., Martens, S., Link, G., Toker, A. and Pfizenmaier, K. (2005). Protein kinase D regulates vesicular transport by phosphorylating and activating phosphatidylinositol-4 kinase IIIbeta at the Golgi complex. *Nat Cell Biol* **7**, 880-6.

Lorenz, M., Yamaguchi, H., Wang, Y., Singer, R. H. and Condeelis, J. (2004). Imaging sites of N-wasp activity in lamellipodia and invadopodia of carcinoma cells. *Curr Biol* **14**, 697-703.

Wille, C., Kohler, C., Armacki, M., Jamali, A., Gossele, U., Pfizenmaier, K., Seufferlein, T. and Eiseler, T. (2014). Protein kinase D2 induces invasion of pancreatic cancer cells by regulating matrix metalloproteinases. *Mol Biol Cell* **25**, 324-36.

Ziegler, S., Eiseler, T., Scholz, R. P., Beck, A., Link, G. and Hausser, A. (2011). A novel protein kinase D phosphorylation site in the tumor suppressor Rab interactor 1 is critical for coordination of cell migration. *Mol Biol Cell* **22**, 570-80.

Table S3: Raw data for AB-FRET experiments

Click here to Download Table S3